Brazilian Journal
of Chemical
Engineering

ISSN 0104-6632
Printed in Brazil
www.abeq.org.br/bjche

Vol. 30, No. 03, pp. 551 - 562, July - September, 2013

MASS TRANSFER OF SO_2 ABSORPTION WITH AN INSTANTANEOUS CHEMICAL REACTION IN A BUBBLE COLUMN

Xiaolei Li[1], Chunying Zhu[1*], Sumin Lu[2] and Youguang Ma[1]

[1]School of Chemical Engineering and Technology, State Key Laboratory of Chemical Engineering,
Phone: +86 (0) 22 2740 4772, Fax: +86 (0) 22 2740 4772, Tianjin University, Tianjin, 300072, China.
E-mail: zhchy971@tju.edu.cn
[2]Department of Material and Chemical, Tianjin Polytechnic University, Tianjin, 300160, China.

(Submitted: April 22, 2012 ; Revised: June 18, 2012 ; Accepted: August 3, 2012)

Abstract - Gas absorption accompanied by an instantaneous irreversible chemical reaction in bubble columns has been analyzed theoretically. A mass transfer model based on the Dankwerts surface-renewal model as well as the penetration theory for surface stretch proposed by Angelo *et al*. was developed, in which the effects of bulk motion and turbulence on mass transfer were taken into account. The analytical expressions for the time-average mass transfer coefficient and the enhancement factor have been obtained. The fast reactive absorption of SO_2 from gas mixtures into aqueous NH_4HCO_3 solution was investigated experimentally in a bubble column reactor to validate the mass transfer model, and the results calculated by the present model agree well with the experimental results.

Keywords: Absorption; Bubble column; Mass transfer; Instantaneous reaction; Enhancement factor.

INTRODUCTION

Gas absorption accompanied by chemical reactions is widely encountered in chemical and allied industries. A number of experimental and theoretical studies on this type of gas absorption process have been reported over the past few decades and many mass transfer models, as well as their corresponding numerical or analytical solutions, have also been developed based on the film theory, the penetration theory or the surface-renewal model (Danckwerts, 1950; Last *et al*., 2002; da Silva *et al*., 2007; Danish *et al*., 2008; Meldon *et al*., 2007; Kakaraniya *et al*., 2007; Jun Yue *et al*., 2012; Zhang *et al*., 2012; Martínez *et al*., 2012). A chemical reaction can be considered to be instantaneous when its rate is much greater than the rate of diffusion. Some typical examples include the removal of hydrogen sulphide by means of sodium hydroxide solution and the absorption of ammonia into sulfuric-acid solution, etc. In fact, many chemical absorption processes can be considered to be instantaneous reactions, e.g., the removal of acidic gases with alkaline solutions, the removal of alkaline gases with acid solutions, etc. For gas absorption accompanied by instantaneous chemical reactions, the solute diffuses from the gas phase into the liquid phase and reacts immediately and completely with the reactant present in the solution, and then a sharp reaction plane parallel to the gas-liquid interface is formed. Danckwerts (1950) developed a mathematical model to describe mass transfer and heat-conduction with a moving boundary for the process of gas absorption accompanied by an instantaneous chemical reaction in an unsteady-state using the film theory. Garg *et al*. (2000) focused on the moving-boundary problem of

---

*To whom correspondence should be addressed gas absorption accompanied by an instantaneous chemical reaction in a limited gas-liquid system. Jun Yue *et al*. (2012) also studied gas absorption with instantaneous reaction in a finite liquid layer. However, because the conventional model for gas reactive absorption generally introduced empirical parameters to reflect the effects of the bulk motion and turbulence, it does not reveal the inherent mechanism of the influence of the bulk motion and turbulence on mass transfer between the gas-liquid phases, especially in a bubble column with very complex two-phase flow behavior. Inspired by this point, Angelo *et al*. (1966) developed the penetration concept in the absence of bulk motion and turbulence and proposed a promising theory called "surface-stretch theory". Jajuee *et al*. (2006) further developed the model by incorporating Dankwerts (1951) surface-renewal model with the penetration theory for surface stretch proposed by Angelo *et al* (1966) and extended the model to liquid-liquid systems.

In this study, a theoretical analysis of gas absorption accompanied by an instantaneous chemical reaction of the type "A + YB = products" is presented taking into account the effects of bulk motion and turbulence. A mass transfer model based on the Dankwerts (1951) surface-renewal model and the penetration theory for surface stretch proposed by Angelo *et al*. (1966) was developed and analytical solutions have been derived. The mass transfer process of the fast reactive absorption of SO_2 into aqueous NH_4HCO_3 solution in a bubble column was experimentally investigated to validate the proposed mass transfer model.

EXPERIMENTAL

A schematic diagram of the experimental setup, which consisted of the mixing gas generation unit, exhaust detection devices and bubble column, is shown in Figure 1. The bubble column was made of stainless steel and was 20 cm in diameter and 45 cm in height.

SO_2 with a volume concentration of 98% (Tianjin Kermel Chemical Reagent Co., Ltd) supplied from a cylinder was diluted with air from the air compressor (Shanghai Jiebao Compressor Manufacture Co., Ltd.). The two kinds of gases were mixed in the gas mixer. Then the air-SO_2 mixture was fed at the bottom of the column and the SO_2 reacted with NH_4HCO_3 (mass purity > 0.995, Tianjin Kermel Chemical Reagent Co., Ltd) immediately in the liquid phase. Air was fed into the bubble column before the experiments. When the system reached stable conditions, valves (3) and (4) on the SO_2 cylinder were opened and the air-SO_2 mixture introduced into the bubble column. The concentration of SO_2 in the exhaust was detected by the flue gas analyzer (Qingdao Minhope electronic instrument Co., Ltd). The liquid was sampled at the bottom of the column in the SO_2 absorption process in order to measure the pH with a digital pH meter. The experiments were carried out at room temperature and repeated three times. The gas flow rates were controlled by rotameters (LZB-type, Tianjin flow Instrument Co., Ltd.) with the measuring range of 0-100 ml·min^{-1} for SO_2 and 0-100 L·min^{-1} for air; the accuracy of rotameters was ±1.5%.

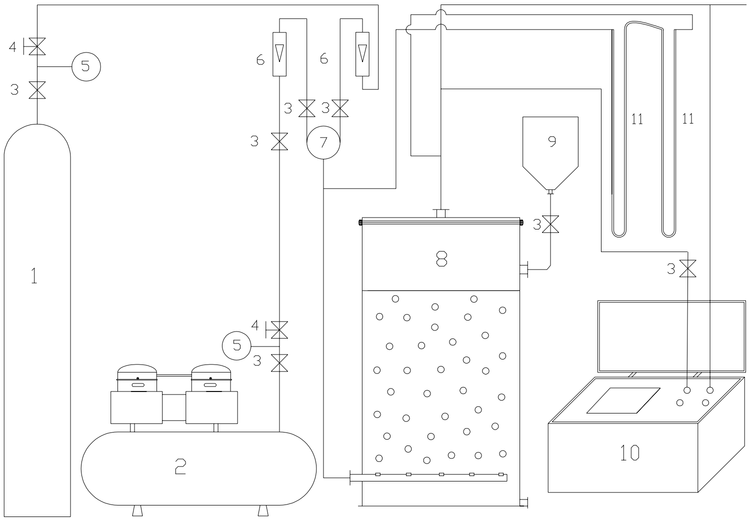

1) Sulfur dioxide cylinder;
2) Air Compressor;
3) Valve;
4) Pressure reducing valve;
5) Manometer;
6) Rotor flow meter;
7) Gas mixer;
8) Bubble column;
9) Feed tank;
10) Flue gas detector;
11) Manometer.

Figure 1: Schematic diagram of the experimental setup

THEORIES

Mass Transfer Model

For gas absorption accompanied by an instantaneous chemical reaction of the type A + YB = products, the heat of reaction could be neglected because of the excellent heat transfer characteristics in the bubble columns when the concentration of the gas-phase reactant is low. It is assumed that diffusion occurs only in the direction perpendicular to the interface. The model describing the process can be stated as follows:

$$\frac{\partial c_A}{\partial \theta} - u_z \frac{\partial c_A}{\partial z} = D_A \frac{\partial^2 c_A}{\partial z^2} \quad \text{for } 0 \le z \le z_\lambda \tag{1}$$

$$\text{IC. } \theta = 0 \Rightarrow c_A = 0 \quad \text{for all z}$$

$$\text{BC. } z = 0 \Rightarrow c_A = A^*,\ z = \lambda \Rightarrow c_A = 0,\ \text{for } \theta > 0$$

$$\frac{\partial c_B}{\partial \theta} - u_z \frac{\partial c_B}{\partial z} = D_B \frac{\partial^2 c_B}{\partial z^2} \quad \text{for } z_\lambda \le z \le \sigma \tag{2}$$

$$\text{IC. } \theta = 0 \Rightarrow c_B = B^* \quad \text{for all z}$$

$$\text{BC. } z = \lambda \Rightarrow c_B = 0,\ z = \sigma \Rightarrow c_B = B^*,\ \text{for } \theta > 0$$

In the position of the reaction plane, the following equation can be obtained:

$$YD_A \frac{dc_A}{dz}\Big|_{z=\lambda} = -D_B \frac{dc_B}{dz}\Big|_{z=\lambda} \tag{3}$$

According to the surface-renewal model of Danckwerts (1951), the surface-age distribution function is given by $\phi(\theta)$:

$$\phi(\theta) = Se^{-S\theta} \tag{4}$$

The film area comprising the elements having ages between θ and $(\theta + d\theta)$ is $\phi(\theta)d\theta$. Let the total area of the surface exposed to the gas be equal to $A(\infty)$ and $A(\theta)$ for the surface areas with ages between θ and $(\theta + d\theta)$. One can then obtain:

$$\frac{dA(\theta)}{A(\infty)} = \phi(\theta)d\theta = Se^{-s\theta}d\theta = -d(e^{-s\theta}) \tag{5}$$

Eq. (5) may be readily integrated and taking $A = A_0$ at $\theta = 0$ gives:

$$A(\theta) = -A_\infty(1 - e^{-s\theta}) + A_0 \tag{6}$$

Consider a small flat element of surface $\Delta x \Delta y$ moving with the fluid bulk velocity, the change in the area of the surface of this flat element with time is:

$$(\frac{\partial A}{\partial \theta}) = \begin{bmatrix} \Delta x(u_y|_{y+\Delta y} - u_y|_y) \\ +\Delta y(u_x|_{x+\Delta x} - u_x|_x) \end{bmatrix} \tag{7}$$

Dividing by $\Delta x \Delta y$ and taking the limit as Δx and Δy approach zero, Eq. (7) may be rewritten as:

$$(\frac{\partial \ln A}{\partial \theta}) = \frac{\partial u_x}{\partial x} + \frac{\partial u_y}{\partial y} \tag{8}$$

For an incompressible fluid, Eq. (8) can take the following form with the aid of the equation of continuity:

$$(\frac{\partial \ln A}{\partial \theta}) = -\frac{\partial u_z}{\partial z} \tag{9}$$

Since the expression on the left-hand side is independent of z, it may be obtained for negligible net transfer across the interface:

$$u_z = -z(\frac{\partial \ln A}{\partial \theta}) \tag{10}$$

To solve Eqs. (1) and (2), we define the following dimensionless variables:

$$Z_1 = z\big/\sqrt{D_A \theta_0} \tag{11}$$

$$Z_2 = z\big/\sqrt{D_B \theta_0} \tag{12}$$

$$T = \theta/\theta_0 \tag{13}$$

$$C_A = c_A\big/A^* \tag{14}$$

$$C_B = c_B\big/B^* \tag{15}$$

where θ_0 is a constant that can be evaluated from the time characteristics of bubble column, the bubble-formation time. Using the dimensionless variables, Eqs. (1) and (2) take the following forms:

$$\frac{\partial C_A}{\partial T} - Z(\frac{\partial \ln A}{\partial T})_{x,y} \frac{\partial C_A}{\partial Z_1} = D_A \frac{\partial^2 C_A}{\partial Z_1^2} \tag{16}$$

IC. $T = 0 \Rightarrow C_A = 0$ for all Z

BC. $Z_1 = 0 \Rightarrow C_A = 1$,

$$Z_1 = \lambda_1 = \lambda \big/ \sqrt{D_A \theta_0} \Rightarrow C_A = 0$$

$$\frac{\partial C_B}{\partial T} - Z(\frac{\partial \ln A}{\partial T})_{x,y} \frac{\partial C_B}{\partial Z_2} = D_B \frac{\partial^2 C_B}{\partial Z_2^2} \tag{17}$$

IC. $T = 0 \Rightarrow C_B = 1$ for all Z

BC. $Z_2 = \lambda_1^{'} = \lambda \big/ \sqrt{D_B \theta_0} \Rightarrow C_B = 0$,

$$Z_2 = \sigma_1 = \sigma \big/ \sqrt{D_B \theta_0} \Rightarrow C_B = 1$$

In order to solve these equations, combinations of the variables are introduced to convert the partial differential Eqs. (16) and (17) to simple differential equations:

$$C_A = C_A(\phi_1) \quad C_B = C_B(\phi_2) \tag{18}$$

where

$$\phi_1 = Z_1 \times G(T) \quad \phi_2 = Z_2 \times G(T) \tag{19}$$

Eqs. (16) and (17) thus become:

$$\frac{d^2 C_A}{d\phi_1^2} + \phi_1 \left[\frac{(\frac{\partial \ln A}{\partial T})_{x,y}}{G^2} - \frac{G^{'}}{G^3} \right] \frac{dC_A}{d\phi_1} = 0 \tag{20}$$

for $0 \le \phi_1 \le \phi_{1,\lambda}$

$$\frac{d^2 C_B}{d\phi_2^2} + \phi_2 \left[\frac{(\frac{\partial \ln A}{\partial T})_{x,y}}{G^2} - \frac{G^{'}}{G^3} \right] \frac{dC_B}{d\phi_2} = 0 \tag{21}$$

for $\phi_{2,\lambda} \le \phi_2 \le \phi_{2,\sigma}$

where $G^{'}$ indicates the partial derivative of G with respect to T at constant Z. It has been assumed that:

$$\left[\frac{(\frac{\partial \ln A}{\partial T})_{x,y}}{G^2} - \frac{G^{'}}{G^3} \right] = \alpha \tag{22}$$

where α is an arbitrary constant. The following assumption was also made:

$$(\frac{\partial \ln A}{\partial T})_{x,y} = F \tag{23}$$

Eq. (22) may be rearranged to:

$$FG - G' = \alpha G^3 \tag{24}$$

Eq. (24) is a Bernoulli equation, which can be put into linear form by the following substitution:

$$G = h^{-1/2} \tag{25}$$

By using Eq. (25), Eq. (24) takes the form:

$$\frac{dh}{dT} = -2Fh + 2\alpha \tag{26}$$

The integrating factor can be introduced:

$$e^{2\int F dT} = e^{2\int \left(\partial \ln A / \partial T \right) dT} = A(T)^2 \tag{27}$$

Combining Eqs (26) and (27), one obtains:

$$A^2 \frac{dh}{dT} = -2hA \frac{dA}{dT} + 2\alpha A^2 \Rightarrow d\left(A^2 h\right) = 2\alpha A \tag{28}$$

Eq. (28) can be integrated:

$$A^2 h = 2\alpha \int_0^T A(T)^2 dT + C_5 \tag{29}$$

Eq. (29) in transformed form becomes:

$$G(T) = A(T) \Big/ \sqrt{2\alpha \int_0^T A(T) dT + C_5} \tag{30}$$

where C_5 is a constant.

Then the solutions of Eqs. (20) and (21) are (Mehra, 1990):

$$C_A = C_1 + C_2 \operatorname{erf}\left(\sqrt{2} \sqrt{\alpha} \phi_1 / 2 \right) \tag{31}$$

$$C_B = C_3 + C_4 \mathrm{erf}\left(\sqrt{2}\sqrt{\alpha}\phi_2/2\right) \tag{32}$$

where C_1, C_2, C_3 and C_4 are constants. If the assumed combinations of variables are successful, equations (23) and (24) should satisfy the initial and boundary conditions of Eqs. (16) and (17).

$$C_A(0) = 1 \quad C_A\left(\phi_{1,\lambda}\right) = 0 \tag{33}$$

$$C_B\left(\phi_{2,\lambda}\right) = 0 \quad C_B\left(\phi_{2,\sigma}\right) = 1 \tag{34}$$

According to the literature (Jajuee *et al.*, 2006), for convenience $\alpha=2$ is taken. Thus, C_5 in Eq. (30) should be zero to satisfy Eq. (33). Combining Eqs. (31) and (33) yields:

$$C_A = 1 - \mathrm{erf}\left(\phi_1\right)/\mathrm{erf}\left(\phi_{1,\lambda}\right) \tag{35}$$

Combining Eqs. (32) and (34) leads to the following relation:

$$\begin{aligned} C_B = &-\frac{\mathrm{erf}\left(\phi_{2,\lambda}\right)}{\mathrm{erf}\left(\phi_{2,\delta}\right) - \mathrm{erf}\left(\phi_{2,\lambda}\right)} \\ &+ \frac{\mathrm{erf}\left(\phi_2\right)}{\mathrm{erf}\left(\phi_{2,\delta}\right) - \mathrm{erf}\left(\phi_{2,\lambda}\right)} \end{aligned} \tag{36}$$

From Eq. (35) one gets:

$$\begin{aligned} &\frac{\partial c_A}{\partial z} = A^* \frac{\partial C_A}{\partial z} = A^* \frac{\partial C_A}{\partial Z}\frac{\partial Z}{\partial z} = \\ &-A^* \cdot \frac{1}{\mathrm{erf}\left(\phi_{1,\lambda}\right)}\frac{2}{\sqrt{\pi}} e^{-\phi_1^2} \cdot \frac{G(T)}{\sqrt{D_A \theta_0}} \end{aligned} \tag{37}$$

From Eq. (36) the following equation can be obtained:

$$\begin{aligned} &\frac{\partial c_B}{\partial z} = B^* \frac{\partial C_B}{\partial z} = B^* \frac{\partial C_B}{\partial Z}\frac{\partial Z}{\partial z} = \\ &B^* \frac{1}{\mathrm{erf}\left(\phi_{2,\delta}\right) - \mathrm{erf}\left(\phi_{2,\lambda}\right)}\frac{2}{\sqrt{\pi}} e^{-\phi_2^2} \cdot \frac{G(T)}{\sqrt{D_B \theta_0}} \end{aligned} \tag{38}$$

At the position of the reaction plane, λ, substituting Eqs. (37) and (38) leads to the function for the change of the position of the reaction with time:

$$\begin{aligned} &\frac{Y\sqrt{D_A}A^*}{\sqrt{D_B}B^*} e^{-\phi_{1,\lambda}^2}\left[\mathrm{erf}\left(\phi_{2,\delta}\right) - \mathrm{erf}\left(\phi_{2,\lambda}\right)\right] \\ &= e^{-\phi_{2,\lambda}^2} \mathrm{erf}\left(\phi_{1,\lambda}\right) \end{aligned} \tag{39}$$

The instantaneous rate of gas absorption for a surface element may be defined by:

$$dN_A = j_{A,z}\frac{dA}{A_\infty} = j_{A,z}\phi(\theta)d\theta \tag{40}$$

where

$$j_{A,z} = -D_A \frac{\partial c_A}{\partial z}\Big|_{z=0} = D_A A^* \frac{\partial C_A}{\partial Z}\Big|_{Z=0}\frac{\partial Z}{\partial z} \tag{41}$$

Hence

$$\begin{aligned} dN_A = &D_A A^* \frac{1}{\mathrm{erf}\left(\phi_{1,\lambda}\right)}\frac{2}{\sqrt{\pi}} \\ &\cdot G(T) \cdot \frac{1}{\sqrt{D_A \theta_0}} \cdot S e^{-S\theta} \cdot d\theta \end{aligned} \tag{42}$$

Eq. (42) can be integrated to get the average flux over the time of exposure per unit area of turbulent surface:

$$\begin{aligned} N_A &= A^* \int_0^\infty \frac{1}{\mathrm{erf}\left(\phi_{1,\lambda}\right)}\frac{2\sqrt{S^2 D_A}}{\sqrt{\pi\theta_0}} \cdot G(T) \cdot e^{-S\theta} \cdot d\theta \\ &= K_L\left(A^* - 0\right) \end{aligned} \tag{43}$$

The time-average mass transfer coefficient can be obtained:

$$K_L = \int_0^\infty \frac{1}{\mathrm{erf}\left(\phi_{1,\lambda}\right)}\frac{2\sqrt{S^2 D_A}}{\sqrt{\pi\theta_0}} \cdot G(T) \cdot e^{-S\theta} \cdot d\theta \tag{44}$$

de Lind van Wijngaarden *et al.* (1986) pointed out that the “equal diffusivities” condition was a severe limitation. Garg *et al.* (2000) derived analytical solutions for the case of equal diffusivities for gas absorption accompanied by an instantaneous chemical reaction in finite gas-liquid systems. The “equal diffusivities” condition is used at $z = \lambda$, the position of reaction plane. From Eq. (39) at $z = \lambda$:

$$\mathrm{erf}\left(\phi_{1,\lambda}\right)=\mathrm{erf}\left(\phi_{2,\lambda}\right) \tag{45}$$

The function for the variation of the position of the reaction plane with time may be obtained:

$$\mathrm{erf}\left(\phi_{1,\lambda}\right)=\frac{Y\sqrt{D_A}A^{*}e^{-1/D_A}\Big/\sqrt{D_B}B^{*}e^{-1/D_B}}{1+Y\sqrt{D_A}A^{*}e^{-1/D_A}\Big/\sqrt{D_B}B^{*}e^{-1/D_B}}\,\mathrm{erf}\left(\phi_{2,\delta}\right) \tag{46}$$

By substituting Eq. (46) into Eq. (44), the mass transfer coefficient is found to be:

$$K_L=\frac{1+\dfrac{Y\sqrt{D_A}A^{*}e^{-1/D_A}}{\sqrt{D_B}B^{*}e^{-1/D_B}}}{\dfrac{Y\sqrt{D_A}A^{*}e^{-1/D_A}}{\sqrt{D_B}B^{*}e^{-1/D_B}}}\sqrt{\frac{D_AS}{\pi}}\int_0^{\infty}\frac{1}{\mathrm{erf}\left(\phi_{2,\delta}\right)}\cdot\frac{2\sqrt{S}}{\sqrt{\theta_0}}G\left(T\right)\cdot e^{-S\theta}\cdot d\theta \tag{47}$$

The expression for the mass transfer coefficient is too complicated to be employed for practical purposes due to the error function in the equation. But when the scale of turbulence is high, Jajuee *et al.* (2006) found that the integrand in Eq. (47) had the value of 2. The scale of turbulence in bubble columns is high; thus the expression of mass transfer coefficient becomes:

$$K_L=\frac{1+Y\sqrt{D_A}A^{*}e^{-1/D_A}\Big/\sqrt{D_B}B^{*}e^{-1/D_B}}{Y\sqrt{D_A}A^{*}e^{-1/D_A}\Big/\sqrt{D_B}B^{*}e^{-1/D_B}}\sqrt{\frac{4D_AS}{\pi}} \tag{48}$$

Harriott (1962) pointed out that the concept of surface-renewal theory could only be expected when $\overline{H}/\sqrt{DS}<0.5$ is met, where $\overline{H}$ is the average distance to which eddies approach the interface. Thus, the distance from the interface to the bulk of the liquid is equal to $\overline{H}$ plus the length of eddies:

$$\delta=\overline{H}+l \tag{49}$$

The length and velocity scales of eddies for isotropic turbulence can be calculated from:

$$l=\left(k^{3}/\varepsilon\right)^{1/4} \tag{50}$$

$$\upsilon=\left(k\varepsilon\right)^{1/4} \tag{51}$$

where k is the kinematic viscosity:

$$k=\mu/\rho \tag{52}$$

ε is the viscous dissipation of energy per unit mass of eddies, which can be calculated from (Wang *et al.*, 2005):

$$\varepsilon=\left(U_g-\frac{\varepsilon_g}{1-\varepsilon_g}U_L\right)g \tag{53}$$

where U_g is the superficial gas velocity, U_L the superficial liquid velocity and ε_g the gas hold-up. For bubble columns with low superficial liquid velocity, U_L can be regarded as zero and the energy dissipation rate can be obtained:

$$\varepsilon=U_gg \tag{54}$$

The fractional rate of surface renewal may be defined as follows (Jajuee *et al.*, 2006):

$$s=\upsilon/l \tag{55}$$

For mass transfer accompanied by chemical reaction, one of the most important parameters is the enhancement factor, defined as the ratio of the time-mean mass flux at the interface with chemical reaction to the time-mean mass flux at the interface without chemical reaction under the same driving force.

$$E=K_L\big/K_L^{*} \tag{56}$$

The time-mean mass flux at the interface without chemical reaction is (Jajuee *et al.*, 2006):

$$K_L^{*}=\sqrt{4D_AS/\pi} \tag{57}$$

Substitution of Eqs. (48) and (57) into Eq. (56) yields:

$$E=1+\frac{1}{Y\sqrt{D_A}A^{*}e^{-1/D_A}\Big/\sqrt{D_B}B^{*}e^{-1/D_B}} \tag{58}$$

Bubble Column Model

In this experiment, low superficial gas velocities were applied, which was in the bubble flow regime. The heat of reaction can be neglected due to the low sulfur dioxide concentration and the excellent heat transfer characteristics of bubble columns. Thus, the mass balance of sulfur dioxide in the gas phase is:

$$\frac{\partial C_{SO_2}}{\partial t} + u_b \frac{\partial C_{SO_2}}{\partial z} = D_g \frac{\partial^2 C_{SO_2}}{\partial z^2} - \frac{K_{L,tol}a}{H\varepsilon_G}\left(HC_{SO_2} - RC_L\right) \qquad (59)$$

The mass balance of sulfur in the liquid phase is:

$$\frac{\partial C_L}{\partial t} = D_L \frac{\partial^2 C_L}{\partial z^2} + \frac{K_{L,tol}a}{1-\varepsilon_G}\left(HC_{SO_2} - RC_L\right) \qquad (60)$$

where the total mass transfer coefficients are given by the following equation:

$$\frac{1}{K_{L,tol}} = \frac{1}{EHK_L^*} + \frac{1}{k_G} \qquad (61)$$

The gas-side volumetric mass transfer coefficient can be calculated from (Cho *et al.* 1988):

$$k_G a = 2.6 \times 10^3 D_G^{0.5} u_b^{0.76} \qquad (62)$$

Before the NH_4HCO_3 is consumed completely, C_L in Eqs. (59) and (60) is zero and E is calculated from Eq. (58). After the NH_4HCO_3 is consumed completely, C_L is the total sulfur concentration in the liquid:

$$C_L = C_{SO_2,L} + C_{HSO_3^-} + C_{SO_3^{2-}} \qquad (63)$$

The following reactions in the bulk liquid should be considered:

$$SO_2 + H_2O = H_2SO_3 = H^+ + HSO_3^- \qquad K_1 = C_{H^+}C_{HSO_3^-} / C_{SO_2} \qquad (64)$$

$$HSO_3^- = H^+ + SO_3^{2-} \qquad K_2 = C_{H^+}C_{SO_3^{2-}} / C_{HSO_3^-} \qquad (65)$$

$$CO_2 + H_2O = H^+ + HCO_3^- \qquad K_3 = C_{H^+}C_{CO_3^{2-}} / C_{HCO_3^-} \qquad (66)$$

$$HCO_3^- = H^+ + CO_3^{2-} \qquad K_4 = C_{H^+}C_{CO_3^{2-}} / C_{HCO_3^-} \qquad (67)$$

$$H_2O = H^+ + OH^- \qquad K_w = C_{H^+}C_{OH^-} \qquad (68)$$

$$NH_4^+ + OH^- = NH_3 + H_2O \qquad K_6 = C_{NH_3} / C_{OH^-}C_{NH_4^+} \qquad (69)$$

The charge balance in the liquid is as follows:

$$C_{NH_4^+} + C_{H^+} = C_{HSO_3^-} + 2C_{SO_3^{2-}} + C_{HCO_3^-} + 2C_{CO_3^{2-}} + C_{OH^-} \qquad (70)$$

Combining Eqs. (63)-(65) leads to:

$$C_{SO_2,L} = RC_L \qquad (71)$$

where

$$R = C_{H^+}^2 / \left(C_{H^+}^2 + K_1 C_{H^+} + K_1 K_2\right) \qquad (72)$$

and E is calculated from (Bokotko *et al.*, 2005):

$$E = 1 + \sqrt{D_{HSO_3^-} K_1 / D_{SO_2}} \Big/ \left(\sqrt{C_{SO_2,L}} + \sqrt{C_{SO_2}}\right) \qquad (73)$$

The chemical reaction equilibrium constants at 25 °C are shown in Table 1. D_{SO_2} $D_{HSO_3^-}$ and $D_{HCO_3^-}$ are respectively 1.83×10^{-9} $m^2\cdot s^{-1}$, 1.545×10^{-9} $m^2\cdot s^{-1}$ and 1.185×10^{-9} $m^2\cdot s^{-1}$ at 25°C (Ebrahimi *et al.*, 2003). The Henry coefficient is 0.8082 atm·kg·mol^{-1} (Ebrahimi *et al.*, 2003).

Table 1: The chemical reaction equilibrium constants

Parameter	**K_1**	**K_2**	**K_3**	**K_4**	**K_5**	**K_6**
Value(mol·kg)$^{-1}$	0.0144	7.0786×10^{-8}	4.3766×10^{-7}	4.6541×10^{-11}	1.0038×10^{-14}	6.5849×10^{-12}

Dispersion coefficient (Meikap *et al.*, 2002), liquid phase:

$$D_L = 0.678 d_R^{1.5} u_b^{0.3} \text{ and } d_R^{1.5} u_b^{0.3} < 400 \tag{74}$$

Dispersion coefficient (Meikap *et al.*, 2002), gas phase:

$$D_g = 50 d_R^{1.5} u_b / \varepsilon_G \tag{75}$$

Bubble rising velocity (Moo-Young *et al.*, 1981):

$$u_b = g\rho d_b^2 / 18\mu \tag{76}$$

where the mean diameter of the bubbles:

$$d_b = 0.18 d_0^{1/2} R_{e0}^{1/3} \tag{77}$$

$$R_{e0} = 4Q\rho_G / \pi d_0 \mu_G \text{ and } R_{e0} < 2000 \tag{78}$$

Gas holdup (Meikap *et al.*, 2002):

$$\varepsilon_g = 0.25\left(d_R^2 \rho_L g / \delta_L\right)^{1/8} \left(g d_R^3 \rho_L^2 / \mu_L^2\right)^{1/12} u_b / \sqrt{g d_R} \tag{79}$$

Interfacial area per unit volume (Meikap *et al.*, 2002):

$$a = 48.7\left(u_b / \mu_L\right)^{0.51} \tag{80}$$

The reactor height was discretized in a spatially uniform grid and the finite difference method was applied. These coupled partial differential equations were solved numerically by using Matlab.

RESULTS AND DISCUSSIONS

In the bubble column model, the liquid-side mass transfer coefficient for the absorption of SO_2 into aqueous NH_4HCO_3 solution was calculated from Eqs. (57) and (58). The comparisons between the calculated results and the experimental results for the fast reactive absorption of SO_2 into aqueous NH_4HCO_3 solution in the bubble column under different operating conditions were made and are shown in Fig. 2-4. It can be seen that the calculated results agree well with the experimental results, which verifies that the mass transfer model based on the aforementioned scheme is reasonable and accurate.

Effect of the Inlet SO_2 Concentration

Figure 2 shows the effect of the inlet SO_2 concentrations on the gas absorption. It can be found from Fig. 2 that the duration time for complete SO_2 removal decreases with the increase of the inlet SO_2 concentration; in the last period of SO_2 absorption, the outlet SO_2 concentration increases more significantly with the increase of the inlet SO_2 concentration. The outlet SO_2 concentration and the pH value of the bulk liquid are plotted against time in Figure 3. It can be seen that the pH value decreased sharply from 6.17 to 3.55 upon absorbing a small amount of SO_2 at the thirtieth minute approximately and the outlet SO_2 concentration increased more and more quickly from 0. This indicated that NH_4HCO_3 in the liquid phase was consumed completely and the absorption process changed from a fast chemical reaction to a weak one. Thus, the absorption rate becomes smaller and the outlet concentration gradually increases.

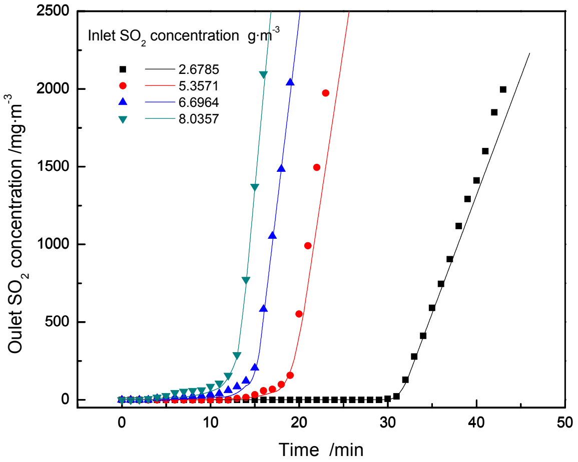

Figure 2: Effect of the inlet SO_2 concentrations on the outlet SO_2 concentrations (concentration of ammonium 0.05%, gas flow rate 20 $L\cdot min^{-1}$). Scatter plots for experimental results and smooth curves for the modeling results.

Effect of the Concentration of NH_4HCO_3

The effect of the concentration of NH_4HCO_3 on the gas absorption was presented in Fig. 4. From Fig. 4, the duration time for complete SO_2 removal increased with the increase of the concentration of NH_4HCO_3. This is because when the concentration of NH_4HCO_3 is high, more SO_2 must be introduced into the system to react completely with NH_4HCO_3. Thus, the duration time for complete SO_2 removal increased with the increase of the concentration of NH_4HCO_3.

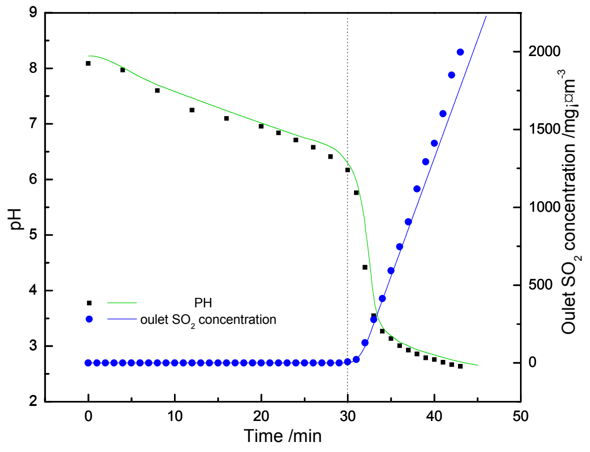

Figure 3: Variation of the outlet SO$_2$ concentrations and pH value varying with time (concentration of the inlet SO$_2$ was 2.6785 g·m^{-3}, concentration of ammonium bicarbonate 0.05%, gas flow rate 20 L·min^{-1}). Scatter plots for experimental results and smooth curves for the modeling results.

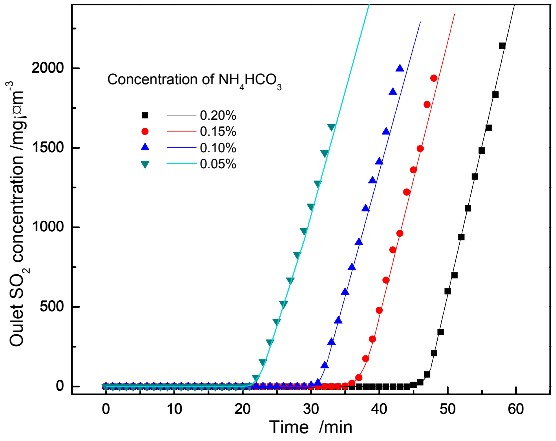

Figure 4: Effect of concentrations of ammonium bicarbonate solution on the outlet SO$_2$ concentrations (inlet concentration of SO$_2$ was 2.6785 g·m^{-3}, gas flow rate 20 L·min^{-1}). Scatter plots for experimental results and smooth curves for the modeling results.

Effect of the Gas Flow Rate

Figure 5 presents the effect of the gas flow rate on the gas absorption. It can be seen from Figure 5 that the duration time for complete SO$_2$ removal decreased rapidly with increasing gas flow rate. In the last period of the SO$_2$ absorption, the outlet SO$_2$ concentrations increased more significantly as the gas flow rate increased. According to Eq. (76), increasing the gas flow rate makes the bubbles' rising velocity higher, which contributes to a very high fractional rate of surface renewal, liquid-side mass transfer coefficient, gas holdup and interfacial area. Thus, NH_4HCO_3 is consumed quickly and the duration time for complete SO$_2$ removal becomes shorter. In the last period of the SO$_2$ absorption, the absorption process is actually water absorbing SO$_2$, and therefore the higher the gas flow rate, the faster the concentration of SO$_2$ in the liquid phase increases. Thus, the outlet SO$_2$ concentrations increase more and more quickly with the increase of the gas flow rate.

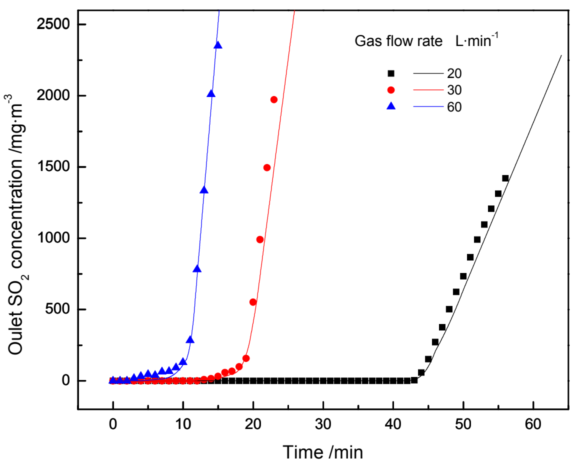

Figure 5: Effect of the gas flow rate on the outlet SO$_2$ concentrations (inlet concentration of SO$_2$ was 5.3571 g·m^{-3}, concentration of ammonium bicarbonate 0.05%. Scatter plots for experimental results and smooth curves for the modeling results.

CONCLUSION

Gas absorption accompanied by an instantaneous irreversible chemical reaction in bubble columns has been studied theoretically and experimentally. A model based on the surface-renewal model and penetration theory has been developed and analytically solved. The analytical expressions for the time-average mass transfer coefficient and the enhancement factor have been derived. The time-average mass transfer coefficient and the enhancement factor are functions of the saturated concentration of the gas-phase reactant in the interface, the concentration of the liquid-phase reactant in the bulk liquid, the diffusion coefficients of the gas-phase and liquid-phase reactants in the liquid and the stoichiometric coefficient of the reaction. The time-average mass transfer coefficient is correlated with the fractional rate of surface renewal and influenced by the bubble rising velocity. The fast reactive absorption of SO_2 into aqueous NH_4HCO_3 solutions with different concentrations in a bubble column was experimentally investigated. An absorption model accompanied by fast chemical reaction has been developed and numerically solved. The prediction results agree well with the experimental results, which validates the mass transfer model proposed.

ACKNOWLEDGMENTS

We gratefully acknowledge the financial support for this project from the National Natural Science Foundation of China (No 21076139), and the Program of Introducing Talents of Discipline to Universities (Grant No B06006).

NOMENCLATURE

a	specific interfacial surface	$m^2 \cdot m^{-3}$
A	exposed area of time-dependent surface	m^2
A_0	initial area of the surface exposed to gas	m^2
A_∞	total area of the surface exposed to gas	m^2
A*	saturation concentration of A	$mol \cdot L^{-1}$
B*	saturation concentration of B	$mol \cdot L^{-1}$
C	molar concentration at the interface	$mol \cdot L^{-1}$
c_A	molar concentration of species A	$mol \cdot L^{-1}$
c_B	molar concentration of species B	$mol \cdot L^{-1}$
C_A	dimensionless concentration profile defined by Eq. (14)	
C_B	dimensionless concentration profile defined by Eq. (15)	
C_i	constant	
C_L	concentration of the total sulfur in the liquid	$mol \cdot L^{-1}$
$C_{SO_2, L}$	concentration of SO_2 in the liquid	$mol \cdot L^{-1}$
D_A	diffusivity of A	$m^2 \cdot s^{-1}$
D_B	diffusivity of B	$m^2 \cdot s^{-1}$
D_g	dispersion coefficient, gas phase	$m^2 \cdot s^{-1}$
D_L	dispersion coefficient, liquid phase	$m^2 \cdot s^{-1}$
D_G	diffusivity in the gas phase	$m^2 \cdot s^{-1}$
D_{SO_2}	diffusivity of SO_2 in the liquid phase	$m^2 \cdot s^{-1}$
$D_{HSO_3^-}$	diffusivity of HSO_3^- in the liquid phase	$m^2 \cdot s^{-1}$
$D_{HCO_3^-}$	diffusivity of HCO_3^- in the liquid phase	$m^2 \cdot s^{-1}$
d_R	column diameter	m
g	gravitational acceleration	$m \cdot s^{-2}$
G	defined by Eq. (19)	
h	defined by Eq. (25)	
H	average distance of approach of eddies to the interface	m
J_A	molar flux of diffusion of species A relative to the molar average velocity	$mol \cdot m^{-2} \cdot s^{-1}$
k_G	gas side mass transfer coefficient	$m \cdot s^{-1}$
k_L	fluid-film mass transfer coefficient	$m \cdot s^{-1}$
K_i	reaction rate constant (i=1, 2, 3, 4, 5, 6)	
K_L	time-average mass transfer coefficient in the liquid phase	$m \cdot s^{-1}$
$K_{L,tol}$	total mass transfer coefficient of SO_2	$m \cdot s^{-1}$
l	length scale of eddies in the viscous dissipation range	m
N_A	overall flux of species A relative to a phase boundary	$mol \cdot m^{-2} \cdot s^{-1}$
R	defined by Eq. (72)	
R_{e0}	the orifice Reynolds number	
S	fractional rate of surface renewal	s^{-1}
T	dimensionless time variable defined by Eq. (13)	
u_g	superficial gas velocity	$m \cdot s^{-1}$
u_l	superficial liquid velocity	$m \cdot s^{-1}$
x	rectangular coordinate	m
y	rectangular coordinate	m
z	rectangular coordinate	m
Z_1	dimensionless position variable defined by Eq. (11)	
Z_2	dimensionless position variable defined by Eq. (12)	

Greek Letters

α	defined by Eq. (22)	
ε	energy dissipation rate per unit mass	$W \cdot kg^{-1}$

ε_G	gas hold-up	
θ	time	s
θ_0	characteristic constant defined for bubble column system	s
κ	kinematic viscosity	$m^2 \cdot s^{-2}$
μ_G	viscosity of gas phase	$kg \cdot m^{-1} \cdot s^{-1}$
μ_L	viscosity of liquid phase	$kg \cdot m^{-1} \cdot s^{-1}$
ρ_G	gas density	$kg \cdot m^{-3}$
ρ_L	liquid density	$kg \cdot m^{-3}$
σ	distance from the interface to the bulk of the liquid	m
σ_1	dimensionless distance from the interface to the bulk of the liquid	
σ_L	surface tension of the liquid	$N \cdot m^{-1}$
υ	molar average velocity; velocity scale of eddies in viscous dissipation range	$m \cdot s^{-1}$
Φ_1	defined by Eq. (19)	
Φ_2	defined by Eq. (19)	

Subscripts

A	gas	phase reactant
B	liquid	phase reactant

REFERENCES

Angelo, J. B., Lightfoot, E. N., Howard, D. W., Generalization of the penetration theory for surface stretch: Application to forming and oscillation drops. AIChE J., 12, 751-760 (1966).

Bokotko, R. P., Hupka, J., Miller, J. D., Flue gas treatment for SO_2 removal with air-sparged hydrocyclone technology. Environ. Sci. Technol., 39, 1184-1189 (2005).

Cho, J. S., Wakao, N., Determination of liquid-side and gas-side volumetric mass transfer coefficients in a bubble column. J. Chem. Eng. Jpn., 21, 576-581 (1988).

da Silva, E. A. B., Souza, D. P., de Souza, A. A. U., de Souza, S. M. A. G. U., Prediction of effective diffusivity tensors for bulk diffusion with chemical reactions in porous media. Braz. J. Chem. Eng., 24, 47-60 (2007).

Danish, M., Sharma, R. K., Ali, S., Gas absorption with first order chemical reaction in a laminar falling film over a reacting solid wall. Appl. Math. Model., 32, 901-929 (2008).

Danckwerts, P. V., Unsteady-state diffusion or heat-conduction with moving boundary. Trans. Faraday Soc., 46, 701-712 (1950).

Dankwerts, P. V., Significance of liquid-film coefficients in gas absorption. Ind. Eng. Chem., 43, 1460-1467 (1951).

de Lind van Wijngaarden, G., Versteeg, G. F., Beenackers, A. A. C. M., Mass-transfer enhancement factors for reversible gas–liquid reactions: Comparison of DeCoursey's and Onda's methods. Chem. Eng. Sci., 41, 2440-2442 (1986).

Ebrahimi, S., Picioreanu, C., Kleerebezem, R., Heijnen, J. J., van Loosdrecht, M. C. M., Rate-based modelling of SO_2 absorption into aqueous $NaHCO_3/Na_2CO_3$ solutions accompanied by the desorption of CO_2. Chem. Eng. Sci., 58, 3589-3600 (2003).

Garg, R., Nair, S., Bhaskarwar, A. N., Mass transfer with instantaneous chemical reaction in finite gas-liquid systems. Chem. Eng. J., 76, 89-98 (2000).

Harriott, P., A random eddy modification of the penetration theory. Chem. Eng. Sci., 17, 149-154 (1962).

Jajuee, B., Margaritis, A., Karamanev, D., Bergougnou, M. A., Application of surface- renewal-stretch model for interface mass transfer. Chem. Eng. Sci., 61, 3917-3929 (2006).

Kakaraniya, S., Kari, C., Verma, R., Mehra, A., Gas absorption in slurries of fine particles: SO_2-$Mg(HO)_2$-$MgSO_3$ system. Ind. Eng. Chem. Res., 46, 1904-1913 (2007).

Last, W., Stichlmair, J., Determination of mass transfer parameters by means of chemical absorption. Chem. Eng. Technol., 25, No. 4, 385-391 (2002).

Martínez, I., Casas, P. A., Simple model for CO_2 absorption in a bubbling water column. Braz. J. Chem. Eng., 29, 107-111 (2012).

Mehra, A., Gas absorption in slurries of finite-capacity microphases. Chem. Eng. Sci., 45, 1525-1538 (1990).

Meikap, B. C., Kundu, G., Biswas, M. N., Modeling of a novel multi-stage bubble column scrubber for flue gas desulfurization. Chem. Eng. J., 86, 331-342 (2002).

Meldon, J. H., Olawoyin, O. O., Bonanno, D., Analysis of mass transfer with reversible chemical reaction. Ind. Eng. Chem. Res., 46, 6140-6146 (2007).

Moo-Young, M., Blanch, H. W., Design of biochemical reactors mass transfer criteria for simple and complex systems. Adv. Biochem. Eng./ Biotechnol., 19, 1-69 (1981).

Wang, T., Wang, J., Jin, Y., Theoretical prediction of flow regime transition in bubble columns by the population balance mode. Chem. Eng. Sci., 60, 6199-6209 (2005).

Yue, J., Rebrov, E. V., Schouten, J. C., Enhancement factor for gas absorption in a finite liquid layer. Part 1: Instantaneous reaction in a liquid in plug flow. Chem. Eng. Technol., 35, No. 4, 679-692 (2012).

Zhang, Y., Zheng, L., Analysis of MHD thermo-solutal Marangoni convection with the heat generation and a first-order chemical reaction. Chem. Eng. Sci., 69, 449-455 (2012).